Critical conductance of two-dimensional chiral systems with random magnetic flux

P. Markoš[1] and L. Schweitzer[2]
[1]*Institute of Physics, Slovak Academy of Sciences, 84511 Bratislava, Slovakia*
[2]*Physikalisch-Technische Bundesanstalt (PTB), Bundesallee 100, 38116 Braunschweig, Germany*
(Received 4 May 2007; published 17 September 2007)

The zero temperature transport properties of two-dimensional lattice systems with static random magnetic flux per plaquette and zero mean are investigated numerically. We study the localization properties and the two-terminal conductance and its dependence on energy, sample size, and magnetic flux strength. The influence of boundary conditions and of the oddness of the number of sites in the transverse direction are also studied. For very long strips of finite width, we find a diverging localization length in the middle of the energy band at $E=0$ and determine its critical exponent $\nu=0.35\pm0.03$. A previously proposed crossover from a power-law dependence to a logarithmic energy dependence can be excluded from our data, at least for energies $|E|>10^{-10}$. For square systems, the sample averaged scale independent critical conductance $\langle g_c\rangle$ turns out to be a function of the amplitude of the flux fluctuations, whereas the variance of the respective conductance distributions appears to be universal. We find a critical conductance $\langle g_c\rangle \simeq 1.49e^2/h$ for the strongest possible disorder.

DOI: 10.1103/PhysRevB.76.115318 PACS number(s): 73.23.−b, 71.30.+h, 72.10.−d

I. INTRODUCTION

The transport properties of charged quantum particles in two-dimensional systems with various types of disorder are of considerable interest in a variety of experimental and theoretical situations. In particular, the presence of a static random magnetic flux with zero mean has been of much concern recently in connection with bond disordered Anderson models with either real or complex hopping terms,[1–10] with the composite-fermion picture of the fractional quantum Hall effect at half-filling,[11,12] the critical behavior at the quantum phase transition of spin-split Landau levels,[13] and with the gauge field theory of high-T_c superconductivity.[14,15] In addition, far-reaching relations between the low energy chiral limit of a quantum chromodynamic (QCD) partition function and a large N limit of the random matrix theory[16,17] as well as between the electrical conductance in disordered media and spontaneous chiral symmetry breaking in QCD have recently become apparent.[18,19]

Concerning the random-flux model, there exists an extensive list of valuable contributions to this intricate problem (see, e.g., Ref. 20 and references therein), but a definite picture started to emerge only recently, at least for quasi-one-dimensional (Q1D) samples.[20] Results for true two-dimensional systems are scarce, and precise numerical estimates are still missing. A consensus has been reached on the notion that all electronic states are localized for such systems, where, in addition to the random magnetic flux, also random diagonal disorder is present.[3,21,22] However, in the absence of diagonal disorder, it has also been shown that the random-flux model with Gaussian distributed and δ-correlated magnetic fields can be mapped onto a nonlinear σ model of unitary symmetry so that all electronic states should be localized.[23] The recognition of a special chiral symmetry that can emerge in systems with an underlying bipartite lattice, so that the eigenvalues appear in pairs $\pm\varepsilon_i$,[24] has considerably augmented our view of the possible situations a random-flux model can assume.[25–29]

Our aim is to investigate a lattice model with static random magnetic fluxes and to numerically calculate the two-terminal conductance and the localization properties for energies close to the band center. We want to study the role of the chiral symmetry and to clarify the possible dependence on boundary conditions (BCs). In addition, we address the influence of an odd or even number of lattice sites. For Q1D systems, we will check the assertion that the Lyapunov exponents do not come in pairs for samples with an even width.[5] We will also look for the crossover proposed for the energy dependence of the localization length.[30] Finally, we will calculate the size dependence of the conductance of square systems and show that at the band center the conductance converges to the critical value $\langle g_c\rangle \simeq 1.49e^2/h$.

The paper is organized as follows. In Sec. III, we study the spectrum of Lyapunov exponents (LEs) in the Q1D limit and for square samples, and discuss how the physical symmetry of the system depends on the boundary conditions, the parity of the width of the system, and energy of the electron. In Sec. IV, we find that $E=0$ is a critical point: the smallest LE does not depend on the width L of the lattice. For L odd and Dirichlet BC, we also calculate the critical exponent for the divergence of the localization length of the two-dimensional system. We find a value $\nu=0.35\pm0.03$, which is close to the critical exponent for the Anderson bond disordered model[4,6] and is also in agreement with the one obtained with a different method for the random-flux model which has been reported recently.[5] For Q1D systems of finite width L, the localization length diverges as $\xi \propto L|\ln(|E|L^{1/\nu})|$. In Sec. V we present our data for the critical two-terminal conductance. Although the scale independent mean value $\langle g_c\rangle$ depends on the strength of the magnetic field fluctuations f, the variance of the corresponding distributions $p_c(g,f)$ turns out to be universal. We also confirm the unusual length dependence of the mean conductance for systems with L odd and DBC.[20] Concluding remarks are given in Sec. VI.

TABLE I. The symmetries of the model Hamiltonian (1) depend on the boundary conditions and on the oddness of the number of sites. In the absence of leads, the possible symmetry classes are unitary (U), chiral unitary (CU), and chiral unitary with an extra eigenvalue that appears at $E=0$ (CU+) (Refs. 20 and 27–29).

	L=odd		L=even	
	DBC$_x$	PBC$_x$	DBC$_x$	PBC$_x$
		L_z=odd		
DBC$_z$	CU+	U	CU	CU
PBC$_z$	U	U	U	U
		L_z=even		
DBC$_z$	CU	U	CU	CU
PBC$_z$	CU	U	CU	CU

II. MODEL AND METHOD

The two-dimensional (2D) motion of noninteracting particles subject to a perpendicular random magnetic field is described by a Hamiltonian

$$\mathcal{H} = -\sum_m [t_x(c^\dagger_{m+a_x}c_m + c^\dagger_{m-a_x}c_m) + t_z(e^{i\alpha_{m,m+a_z}}c^\dagger_{m+a_z}c_m + e^{-i\alpha_{m,m-a_z}}c^\dagger_{m-a_z}c_m)], \quad (1)$$

with nearest neighbor hopping, defined on the sites m of a 2D square lattice, where the width L (x direction) and the length L_z (z direction) of the sample are measured in units of the lattice constant a. The value of the hopping term in the x direction is $t_x=1$ if not stated otherwise, and the energy is given in units of $t_z=1$. The operators $c^\dagger_m$ and c_m create or annihilate a Fermi particle at site m, respectively. The complex hopping terms are chosen such that the magnetic flux (in units of the flux quantum h/e) through an individual plaquette is given by the sum of the random Peierls phases along the two bonds in the z direction, $2\pi\phi_m=\alpha_{m,m+a_z}-\alpha_{m+a_x,m+a_z}$. The random fluxes are distributed uniformly according to $-f/2\leqslant\phi_m\leqslant f/2$, where $0<f\leqslant 1$, with probability density $p(\phi_m)=1/f$ so that its second moment is $f^2/12$, and the average magnetic flux through the system is zero. The randomness is maximal for $f=1$.

Without attached leads, the model (1) exhibits chiral unitary symmetry for Dirichlet boundary conditions in both directions. The chirality is destroyed when periodic boundary conditions are imposed along any direction, provided the number of sites in this direction is odd. Table I summarizes the various situations. The chiral symmetry is always broken by an additional on-site disorder.

In the following, we study numerically the quantum transport of electrons with energy E through the 2D system defined by the Hamiltonian (1). For a given length of the system L_z, we calculate the dimensionless two-terminal conductance via the relation[31]

$$g = \mathrm{Tr}\{T^\dagger T\} = \sum_i^N \frac{1}{\cosh^2(x_i/2)}. \quad (2)$$

In Eq. (2), T is the transmission matrix and the x_i parametrizes its eigenvalues. The electrons propagate in the z direction, and N is the number of open channels. Dirichlet (DBCs) or periodic (PBCs) boundary conditions are imposed in the transversal direction. In the limit of $L_z/L\to\infty$, the parameters x_i converge to the quantities $z_i(L_z/L)$,[32,33] where z_i is the ith LE which characterizes the exponential decrease of the wave function of Q1D systems. Oseledec proved[34] the convergence for the eigenvalues of the transfer matrix, $z_i=\lim_{L_z/L\to\infty}z_i(L_z/L)$. For sufficiently large L_z/L, the $z_i(L_z/L)$ are self-averaging quantities. The smallest positive LE z_1 is related to the localization length and represents the key parameter of finite-size scaling.[35,36]

Since the calculation of the transmission probability requires two semi-infinite (ideal in our case) leads attached to the left and to the right of the sample, the boundary conditions in the propagation (z) direction are neither PBC nor DBC. We expect, however, that the boundary conditions in the transversal (x) direction affect the transport properties of the system considerably.

Our data, both for the conductance and for the parameters x_i, support the conjecture that (i) the system possesses chiral unitary symmetry only at the band center $E=0$ for DBC, and for PBC with L even. The chirality of the $E=0$ state is confirmed by our data for the parameters x_i. In particular, we find that the probability $p(x_1)$ does not decrease to zero when $x_1\to 0$. We will discuss later that this behavior is typical for the chiral symmetry class. (ii) There exists a critical point at the band center for L odd and DBC. Since this critical point is due to the chiral symmetry of the model, we expect the criticality also for L even. This expectation is supported by our numerical data for the smallest LE z_1. For L odd and PBC, the critical state at $E=0$ should disappear due to the unitary symmetry.

III. LYAPUNOV EXPONENTS

Figure 1 shows the spectrum of Lyapunov exponents $|z_i|$ for Q1D systems with Dirichlet and periodic BCs in the transverse direction and with either odd ($L=65$) or even ($L=64$) system width. For L even, the spectrum is degenerate at the band center for both Dirichlet and periodic BCs:

$$|z_{2i-1}| = |z_{2i}| = c[i-1/2] \quad (L \text{ even}). \quad (3)$$

For L odd, we obtain at the band center that

$$|z_i| = \begin{cases} c\ \mathrm{Int}[i/2] & (L \text{ odd, DBC}) \\ (c/2)[i-1/2] & (L \text{ odd, PBC}). \end{cases} \quad (4)$$

From Fig. 1 and later from Fig. 8, we see that $c\approx 2.68$. As is shown in Fig. 1, the degeneracy is removed for nonzero energy. In the transfer matrix method, we calculate only *positive* Lyapunov exponents. Since the LE appear in pairs, we also have doubly degenerate LE $(-z_i,-z_i)$ in the negative part of the spectra.

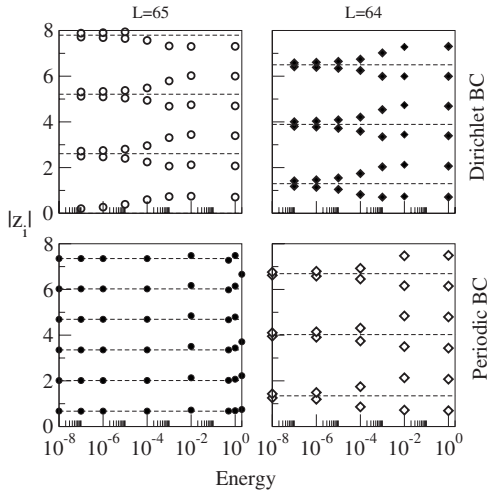

FIG. 1. The energy dependence of the spectrum of Lyapunov exponents $|z_i|$ of the transfer matrix. Dirichlet and periodic BCs are imposed in the transversal direction, and $f=1$. Left: $L=65$, right: $L=64$. Dashed lines indicate the values of the Lyapunov exponents for $E=0$. Note that $z_1=0$ for L odd and Dirichlet BC.

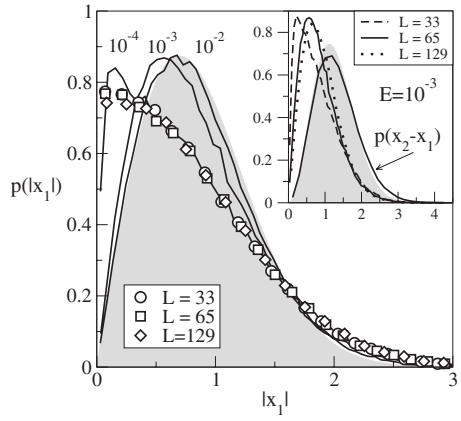

FIG. 2. The probability distribution $p(|x_1|)$ for $E=0$ and $L=33$, 65, and 129 (data points). Solid lines are $p(x_1)$ for $L=65$ and $E=10^{-4}$, 10^{-3}, and 10^{-2} (from the left). The last distribution is compared with the Wigner surmise $\langle x_1\rangle W_1(x_1)=\frac{\pi}{2}s\exp-\frac{\pi}{4}s^2$, where $s=x_1/\langle x_1\rangle$. The inset shows $p(x_1)$ for $E=10^{-3}$ and $L=33$, 65, and 129. Also shown is the distribution $p(x_2-x_1)$ for $E=10^{-3}$ and $L=129$, which is almost identical with the Wigner surmise $\langle x_1\rangle W_2(x_1)=\frac{32}{\pi^2}s^2\exp-\frac{4}{\pi}s^2$ for unitary ensemble.

While the form of the spectrum of LE for odd L and PBC is typical for unitary symmetry,[37] the degeneracy of the spectra, observed in all three other cases, indicates chiral symmetry.[20,27,28]

For DBC, the chirality is confirmed also by the analysis of the distribution of parameters x_i, calculated for finite length L_z. Since we are able to calculate only the absolute value of the LE, we cannot distinguish from the present data whether the system possesses chiral unitary (CU) or unitary (U) symmetry. Fortunately, we can estimate the physical symmetry from the analysis of the distribution of the parameter x_i, calculated for systems of finite length L_z.

As discussed in Refs. 20 and 28, for weak disorder, the probability distribution $p(\{x\})$ is determined by the Dorokhov-Mello-Pereyra-Kumar equation[38,39]

$$\ell\frac{\partial p}{\partial L_z}=\frac{1}{2N}\sum_{j=1}^{N}\frac{\partial}{\partial x_j}\left[J\frac{\partial}{\partial x_j}(J^{-1}p)\right]. \tag{5}$$

Here, ℓ is the mean free path and J is the Jacobian

$$J=\begin{cases}\Pi_{k>j}|\sinh(x_j-x_k)|^2 & (\mathrm{CU})\\ \Pi_{k>j}|\sinh^2 x_j-\sinh^2 x_k|^2\Pi_k|\sin(2x_j)| & (\mathrm{U}).\end{cases} \tag{6}$$

The main consequence of the absence of the repulsion term $\sin(2x_i)$ in the Jacobian (6) is that the spectrum of x_i spans over the entire real axis: the x_i can be both positive and negative when the system possesses chiral unitary symmetry. In the ordinary unitary systems, all values of x_i are positive, being reflected from the origin by an additional term in the Jacobian. Clearly, in the case of unitary symmetry, $p(x_1)\to 0$ when $x_1\to 0$, but $p(x_1=0)$ is nonzero in the case of chiral symmetry. Since we are not able to calculate the sign of the parameters x_i for a given sample, we plot in Fig. 2 the distribution of the *absolute value* $|x_1|$. Dirichlet BCs are imposed in the transversal direction. For $E=0$, the distribution does not depend on the system size. If x_1 possesses both positive and negative values, the distribution $p(x_1)$ is Gaussian with a mean value $\langle x_1\rangle=0$. This agrees with our data for the Q1D systems, where we find $z_1=0$. Therefore, we conclude that the system possesses chiral symmetry.

However, the form of the distribution $p(x_1)$ changes qualitatively when the energy differs from zero. As is shown in Fig. 2, already for $E=10^{-4}$ the distribution $p(|x_1|)$ decreases to zero when $|x_1|\to 0$. This confirms that the Jacobian given by Eq. (6) contains also the repulsion term $\propto\sin(2x)$. Consequently, the system changes the symmetry from chiral unitary to unitary and all parameters x_i become positive. As shown in Fig. 2, the distribution $p(x_1)$ converges to the Wigner surmise W_1 when either E or L increases. Also, the distribution of differences x_2-x_1 converges to the Wigner surmise W_2. This behavior of $p(x_1)$ and $p(x_2-x_1)$ is typical for the unitary universality class.[37]

In the case of L odd and PBC in the transverse direction, the symmetry changes to unitary and the critical point at $E=0$ disappears. The transfer matrix algorithm does not enable us to calculate the parameters x_i for $E=0$ and PBC due to the $k_z=0$ eigenmode of the transfer matrix in unperturbed leads. This mode disappears either when $E\neq 0$ or when an anisotropy in the hopping terms is applied. Using a small anisotropy in the x direction, $t_x=0.99$, we confirmed that the statistics of $p(x_1)$ and $p(x_2-x_1)$ follow the Wigner surmises also at the band center. Figure 3 shows the respective distributions $p(x_1)$ to be W_1 and $p(x_2-x_1)$ to be W_2. This is in contrast to the situation with DBC, where the distribution changes qualitatively on approaching $E=0$.

In the case of L even, the analysis is more difficult since we expect the mean values of the first two parameters x_1 and x_2 to have the same absolute value but with an opposite sign. So, we cannot distinguish between $|x_1|$ and $|x_2|$ in our analysis of a given sample. To overcome this problem, we calculate for N_{stat} realizations the common probability distribution,

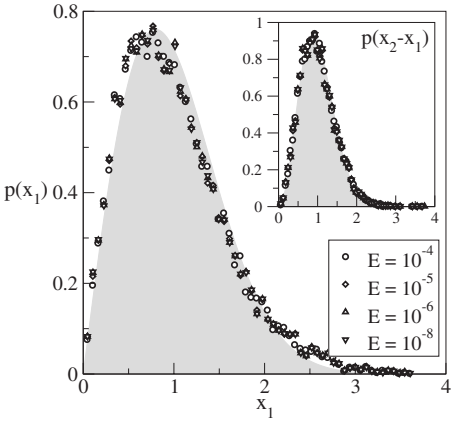

FIG. 3. The probability distribution $p(x_1)$ for a system with PBC at $E=0$. The system size is 65×66 and $t_x=0.99$. $p(x_1)$ agrees well with the Wigner surmise for orthogonal ensemble and $p(x_1-x_2)$ (shown in the inset) for unitary ensemble (Ref. 37).

$$\tilde{p}_{12}(x) = \frac{1}{N_{\text{stat}}} \sum_{j}^{N_{\text{stat}}} \delta(x - |x_1|) + \delta(x - |x_2|), \tag{7}$$

of the parameters $|x_1|$ and $|x_2|$ for a square system $L\times L$ with $L=66$ and DBC in the transversal direction (Fig. 4). We see that the probability $\tilde{p}_{12}(x)$ (shown by the shaded area) is nonzero when $x\to0$. We expect, therefore, that the distribution

$$p_{12}(x) = \frac{1}{N_{\text{stat}}} \sum_{j}^{N_{\text{stat}}} \delta(x - x_1) + \delta(x - x_2) \tag{8}$$

is of the form

$$p_{12}(x) = \frac{1}{\sqrt{2\pi\sigma}} [e^{-(x - \langle x_1\rangle)^2/2\sigma} + e^{-(x + \langle x_1\rangle)^2/2\sigma}]. \tag{9}$$

This expectation is confirmed also by Fig. 5, which shows how the probability distribution changes when the system length increases.

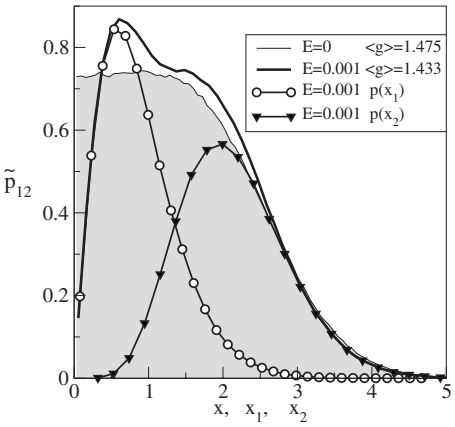

FIG. 4. The probability distribution $\tilde{p}_{12}$, defined by Eq. (7), for $E=0$ (shaded area) and for $E=0.001$. The size of the system is 66×66. Dirichlet BCs are used in the transversal direction. Also shown are distributions $p(x_1)$ and $p(x_2)$ for $E=0.001$. Note that $p\to0$ when $x\to0$. This confirms that the system possesses different physical symmetries for $E=0$ and $E\neq0$, in agreement with Ref. 20.

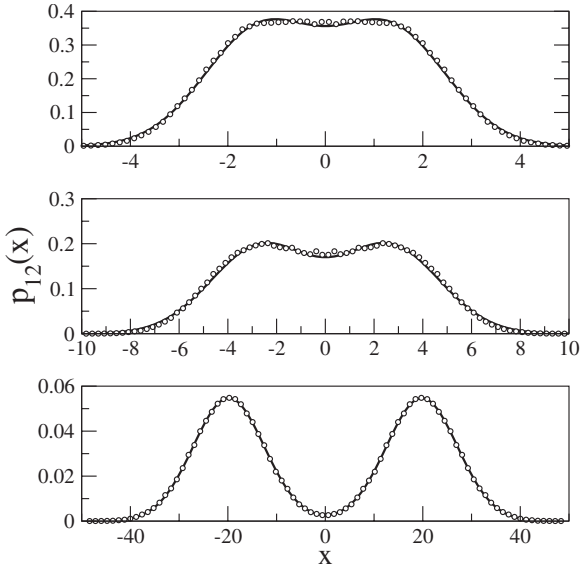

FIG. 5. The distribution $p_{12}(x)$ for systems with even width $L=66$. The lengths of the system are $L_z=66$ (top), $L_z=132$ (middle), and $L_z=1000$ (bottom). The solid line is the fit of $p_{12}(x)$, given by Eq. (9).

For square systems, we obtain the distribution shown in Fig. 4, which, in the limit of $L_z/L\to\infty$, transforms into two Gaussian peaks. For longer systems, $p(x_1,x_2)$ develops into two isolated Gaussian peaks centered around the mean values, $\langle x_1\rangle=-\langle x_2\rangle$. In analogy to the odd L case, a nonzero energy breaks the chiral symmetry also in the even L situation. A similar statistic was observed also for PBC with small anisotropy (not shown), which confirms the existence of the chiral symmetry also for L even and PBC.

We conclude that the random-flux model with Dirichlet BCs possesses at the band center $E=0$ a chiral unitary symmetry. The spectrum of the Lyapunov exponents is given by the relations

$$z_i = c(-1)^{i+1}\,\text{Int}[(i+1)/2] \quad (L \text{ even}) \tag{10}$$

and

$$z_i = c(-1)^{i}\,\text{Int}[i/2] \quad (L \text{ odd, DBC}), \tag{11}$$

in agreement with previous theoretical considerations.[20]

IV. CRITICAL REGIME AND EXPONENT

Since $z_1\equiv0$ for $E=0$, L odd, and DBC in the transversal direction, the system is in the critical regime with a diverging correlation length

$$\xi \propto |E|^{-\nu} \quad (2\text{D}). \tag{12}$$

To estimate the critical exponent ν, we calculate z_1 as a function of energy E and of the system width L. We expect, in agreement with the single parameter scaling,[36,40] that z_1 is a function of the ratio $L/\xi(E)$ only. As is shown in Fig. 6, all numerical data can be fitted by the universal function

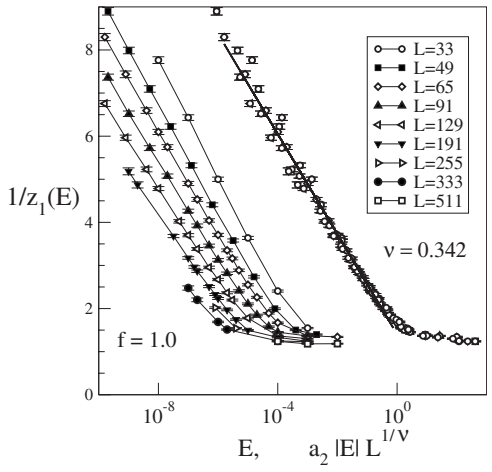

FIG. 6. The energy dependence of the spectrum of Lyapunov exponent z_1 of the transfer matrix. Hard wall boundary conditions are imposed in the transversal direction and $f=1$. The width of the system is given in the legend. The data scale to the universal curve on the right hand side, described by Eq. (13), with critical exponent $\nu=0.342$ and $a_2=0.05$.

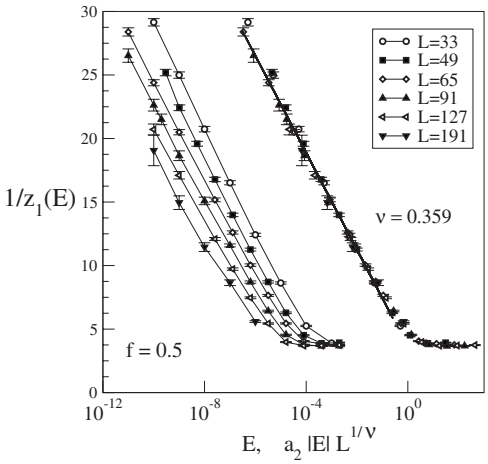

FIG. 7. The energy dependence of the spectrum of Lyapunov exponents z_1 of the transfer matrix. Hard wall boundary conditions are imposed in the transversal direction and the flux strength is $f=0.5$. The width of the system is given in the legend. The data scale to the universal curve (right hand side) given by Eq. (13), with $\nu=0.359$ and $a_2=0.30$.

$$z_1(E,L) = \frac{a_1}{|\ln(a_2|E|L^{1/\nu})|}, \tag{13}$$

with three fitting parameters a_1, a_2, and ν. From the scaling analysis, we observed that

$$\nu = 0.35 \pm 0.03. \tag{14}$$

More detailed information of the analysis is presented in Table II. To estimate the accuracy of our result, we repeated the scaling analysis with reduced input data sets. A similar value of the critical exponent was obtained also for systems with weaker magnetic flux disorder $f=0.5$ (see Fig. 7). Due to the smaller values of z_1, we have to simulate much longer Q1D systems in order to get data with reasonable accuracy.

TABLE II. Numerical estimate of the critical exponent ν for two different strengths of the random-flux amplitudes, $f=1.0$ and $f=0.5$. Only data for $L>L_{\min}$ and with $z_1<z_{1\,\max}$ are considered in the scaling analysis. $F_{\min}$ is obtained from the minimum of the fitting function; N_{data} is the number of data. The accuracy of the critical exponent in each fitting procedure is of the order of 10^{-3}.

$L_{\min}$	$z_{1\,\max}$	ν	$F_{\min}/N_{\text{data}}$
		$f=1.0$	
33	0.62	0.342	20/69
33	0.52	0.336	10/58
65	0.62	0.348	13/55
65	0.52	0.342	7/49
91	0.62	0.368	7/39
91	0.52	0.355	4/35
91	0.45	0.341	3/30
91	0.40	0.329	2/25
		$f=0.5$	
33	0.15	0.359	4/36
33	0.20	0.384	11/42
33	0.25	0.372	26/45

Although the calculated values of ν for $f=0.5$ differ slightly from those obtained for $f=1.0$, we do not interpret this difference as a nonuniversality of the critical exponent.[6] Rather we assume that this difference is due to the limited accuracy of our numerical data and/or fitting procedure. Indeed, as shown in Table II, the estimated value of the critical exponent depends on the choice of the input ensemble defined by $z_{1\,\max}$ and $L_{\min}$, and decreases slightly when larger values of z_1 are excluded.

We did not find any crossover from a power-law dependence to a more complicated E dependence of the localization length for two dimensions as proposed in Ref. 30 and discussed in Refs. 6 and 9. Our numerical data cannot be fitted to the one parameter scaling function $z_1(E,L)=z_1(L/\xi)$ with a localization length $\xi \propto \exp\sqrt{\ln(E_0/E)}$.[30] Since we analyze a very narrow energy interval around the band center (as small as $|E| \sim 10^{-10}$), we do not expect that the crossover from the observed power-law dependence to the proposed logarithmic energy dependence of the localization length exists in our situation.

Since z_1 determines the localization length of the Q1D system, $\xi=2/z_1$, we see from Eq. (13) that the localization length diverges as

$$\xi_L(E) \propto L|\ln(a_2|E|L^{1/\nu})| \quad \text{(Q1D)}, \quad E \to 0, \tag{15}$$

for a given system width L. A logarithmic divergence is typical for Anderson bond disordered models.[41,42]

While the existence of the critical state at $E=0$ for L even is commonly accepted,[3] we do not expect the same for L odd and PBC, since the system possesses unitary symmetry in this case. To describe the property of the $E=0$ state, we plot in Fig. 8 the L dependence of the smallest LE z_1 for L even

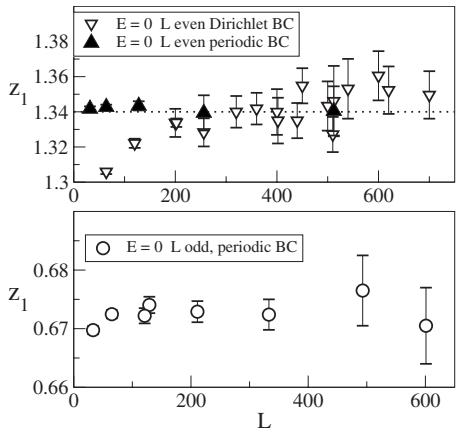

FIG. 8. The smallest Lyapunov exponent z_1 as a function of the system width L for L even (top) and L odd (bottom). The data confirm that z_1 does not depend on the system width. This either implicates the existence of a critical point at the band center in all three cases or a finite-size effect due to the limited system size.

(both Dirichlet and periodic BCs) and L odd (PBC). In all three situations, we do not observe any L dependence of the smallest LE z_1. We believe that this indicates that the localization lengths considerably exceed the available system sizes so that no final conclusions can be reached.

The scaling analysis is very difficult in the case of L even. As is shown in Fig. 9, the L dependence of z_1 is highly nontrivial for nonzero energies, in accordance with Ref. 5. The scaling seems to work only in the limit of $L \to \infty$. We disagree on the observation[5] that the LEs at $E=0$ do not come in degenerate pairs. In contrast, we find the difference between the two LEs to be smaller than the accuracy of our calculations.

The criticality of the $E=0$ state for the Dirichlet BCs will be supported also by the size dependence of the mean conductance, discussed in the next section.

V. CONDUCTANCE

Figure 10 shows the size dependence of the sample averaged critical conductance $\langle g_c \rangle$ for square systems $L \times L$ (L odd) and three values of the randomness strength f. The energy is $E=0$, and Dirichlet BCs are considered. Our data confirm that $\langle g \rangle$ converges to an L independent critical value $\langle g_c \rangle$, which, however, does depend on the strength of the randomness f. For the largest possible disorder $f=1$, we obtain $\langle g_c \rangle = 1.49$, a value larger than the 2D symplectic case.[43] Figure 11 shows the f dependence of the mean conductance for squares of size 257×257. It also shows that the variance var $g = \langle g^2 \rangle - \langle g \rangle^2$ is universal and independent of f. We find a value var $g \approx 0.187$, which is in agreement with those obtained earlier by Ohtsuki *et al.*[44] and Furusaki.[3] We observe, however, an increase of var g for very small f, which can be explained by finite-size effects due to a large mean free path.

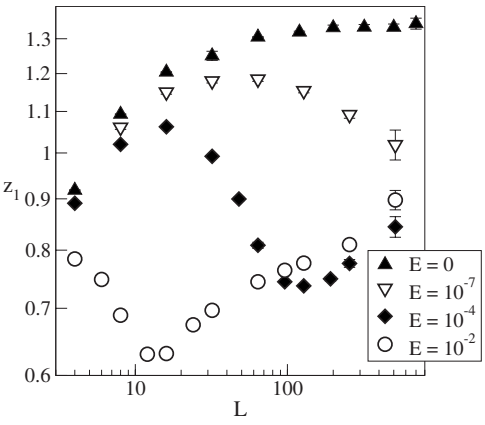

FIG. 9. The L dependence of the smallest Lyapunov exponent z_1 for L even and for various values of the energy E. The nonmonotonous L dependence disables the scaling analysis in this case. Our data are consistent with Fig. 1 of Ref. 5.

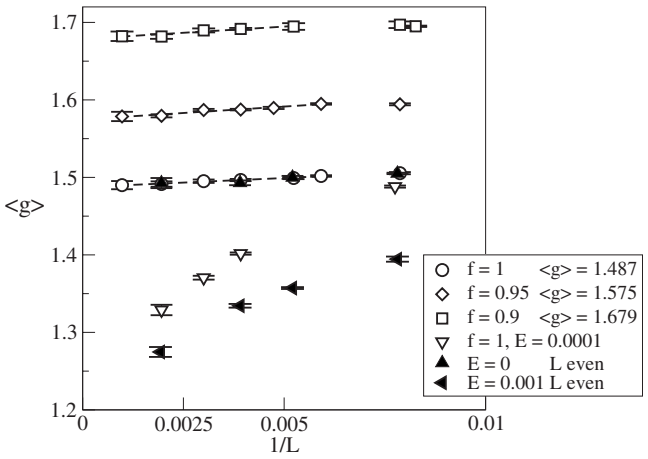

FIG. 10. The critical value of the mean conductance $\langle g_c \rangle$ as a function of the system's size $L \times L$ with L odd (open symbols) and L even (full symbols) at $E=0$ with DBC, and various strengths of the random field f. The data show that the critical conductance does not depend on the parity of L, but depends on f. For completeness, we also add data for $E=0.0001$ (L odd) and $E=0.001$ (L even) to show that the conductance decreases with L when $E \neq 0$, indicating that the system is in the localized regime in the limit of $L \to \infty$.

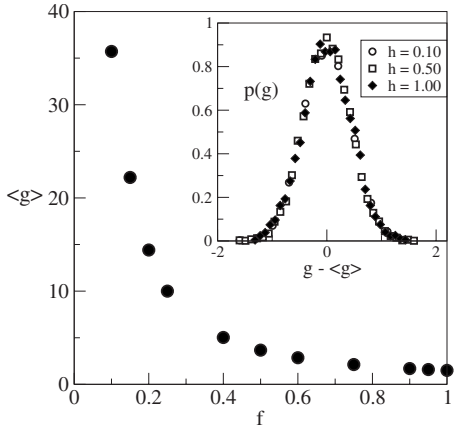

FIG. 11. The critical value of the mean conductance $\langle g_c \rangle$ for square samples 257×257 at $E=0$ and various values of the random field f. Dirichlet BCs are used in the transversal direction. The inset shows the probability distribution $p(g - \langle g \rangle)$ for three different values of f. The width of the distribution var $g \approx 0.187$ does not depend on f.

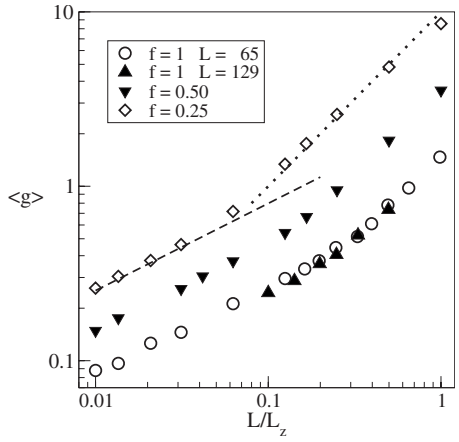

FIG. 12. The length dependence of the mean conductance $\langle g \rangle$ for Q1D systems. The system's width is $L=65$ and the energy $E=0$. One clearly sees the crossover from the $1/L$ (dotted line) to $1/\sqrt{L_z}$ (dashed line) dependence predicted by Ref. 20.

We also plot in Fig. 10 the size dependence of the mean conductance for squares with even L. Within the obtained accuracy, $\langle g_c \rangle$ does neither depend on the parity of L nor on the boundary conditions, in agreement with Ref. 3. Contrary to the band center, the conductance decreases always with increasing system size whenever the energy lies outside the band center.

We also analyzed the length dependence of the mean conductance $\langle g \rangle$ and of the mean of the logarithm of the conductance $\langle \ln g \rangle$ for systems with hard wall transversal boundary conditions and $E=0$. Since $\langle x_1 \rangle \equiv 0$ in this case, we expect that the system possesses an infinite localization length also in the Q1D limit.[20] Therefore, the mean conductance $\langle g \rangle$ should not decrease exponentially when the system length increases.

Our results shown in Fig. 12 confirm the relations predicted theoretically[20]

$$\langle g \rangle = L\ell/L_z \tag{16}$$

and

$$\langle g \rangle = \sqrt{2L\ell/\pi L_z} \tag{17}$$

in the limit of $\langle g \rangle \approx 1$ and $\langle g \rangle \ll 1$, respectively.

VI. SUMMARY

We investigated two-dimensional electron systems with static random magnetic flux and showed numerically that the transport properties depend on the parity of the system's width L and on the transverse boundary conditions. For Dirichlet boundary conditions, we confirmed by the analysis of the statistical properties of the quantities x, which parametrize the eigenvalues of the transmission matrix, that the system possesses chiral unitary symmetry at the band center. The chirality exists in the case of Dirichlet boundary conditions for both L odd and even, and for periodic BC for L even only. However, the chirality is always broken when the energy of the electron is nonzero.

In the case of chiral unitary symmetry, the 2D system with random magnetic flux possesses a critical point at the band center. We found that the localization length diverges $\propto |E|^{-\nu}$ when $E \to 0$, and calculated the critical exponent $\nu \approx 0.35$ for L odd and Dirichlet BCs. Our data do not confirm the existence of the crossover from the power-law dependence to the logarithmic energy dependence of ξ predicted by Ref. 30.

We also calculated the critical conductance of 2D systems. At the band center, the mean conductance $\langle g \rangle$ converges to a size-independent critical value for both L odd and L even. Although the critical conductance does depend on the strength of the randomness, the fluctuations of the conductance appear to be universal. For nonzero energy, the mean conductance decreases with the system size, indicating a localized regime. Finally, for the Q1D systems with odd system width and Dirichlet BCs, we confirmed the nontrivial length dependence of the mean conductance, proposed theoretically in Ref. 20.

ACKNOWLEDGMENTS

P.M. thanks grants from APVV Project No. 51-003505 and VEGA Project No. 2/6069/26, and PTB for hospitality.

[1] P. A. Lee and D. S. Fisher, Phys. Rev. Lett. **47**, 882 (1981).
[2] T. Sugiyama and N. Nagaosa, Phys. Rev. Lett. **70**, 1980 (1993).
[3] A. Furusaki, Phys. Rev. Lett. **82**, 604 (1999).
[4] V. Z. Cerovski, Phys. Rev. B **62**, 12775 (2000).
[5] V. Z. Cerovski, Phys. Rev. B **64**, 161101(R) (2001).
[6] A. Eilmes, R. A. Römer, and M. Schreiber, Physica B **296**, 46 (2001).
[7] S. N. Evangelou and D. E. Katsanos, J. Phys. A **36**, 3237 (2003).
[8] A. M. García-García and K. Takahashi, Nucl. Phys. B **700**, 361 (2004).
[9] A. Eilmes and R. A. Römer, Phys. Status Solidi B **241**, 2079 (2004).
[10] A. M. García-García and E. Cuevas, Phys. Rev. B **74**, 113101 (2006).
[11] V. Kalmeyer and S.-C. Zhang, Phys. Rev. B **46**, 9889 (1992).
[12] B. I. Halperin, P. A. Lee, and N. Read, Phys. Rev. B **47**, 7312 (1993).
[13] D. K. K. Lee and J. T. Chalker, Phys. Rev. Lett. **72**, 1510 (1994).
[14] N. Nagaosa and P. A. Lee, Phys. Rev. Lett. **64**, 2450 (1990).
[15] B. L. Altshuler and L. B. Ioffe, Phys. Rev. Lett. **69**, 2979 (1992).
[16] E. V. Shuryak and J. J. M. Verbaarschot, Nucl. Phys. A **560**, 306 (1993).
[17] A. M. García-García and J. J. M. Verbaarschot, Nucl. Phys. B **586**, 668 (2000).
[18] A. M. García-García and J. C. Osborn, Phys. Rev. Lett. **93**, 132002 (2004).
[19] A. M. García-García and J. C. Osborn, Phys. Rev. D **75**, 034503 (2007).

[20] C. Mudry, P. W. Brouwer, and A. Furusaki, Phys. Rev. B **59**, 13221 (1999).
[21] M. Batsch, L. Schweitzer, and B. Kramer, Physica B **249–251**, 792 (1998).
[22] H. Potempa and L. Schweitzer, Ann. Phys. **8**, SI-209 (1999).
[23] A. G. Aronov, A. D. Mirlin, and P. Wölfle, Phys. Rev. B **49**, 16609 (1994).
[24] M. Inui, S. A. Trugman, and E. Abrahams, Phys. Rev. B **49**, 3190 (1994).
[25] R. Gade and F. Wegner, Nucl. Phys. B **360**, 213 (1991).
[26] R. Gade, Nucl. Phys. B **398**, 499 (1993).
[27] J. Miller and J. Wang, Phys. Rev. Lett. **76**, 1461 (1996).
[28] P. W. Brouwer, C. Mudry, B. D. Simons, and A. Altland, Phys. Rev. Lett. **81**, 862 (1998).
[29] A. Altland and B. D. Simons, J. Phys. A **32**, L353 (1999).
[30] M. Fabrizio and C. Castelliani, Nucl. Phys. B **583**, 542 (2000).
[31] E. N. Economou and C. M. Soukoulis, Phys. Rev. Lett. **46**, 618 (1981).
[32] J.-L. Pichard, N. Zanon, Y. Imry, and A. D. Stone, J. Phys. (France) **51**, 587 (1990).
[33] P. Markoš, J. Phys.: Condens. Matter **7**, 8361 (1995).
[34] V. I. Oseledec, Trans. Mosc. Math. Soc. **19**, 197 (1968).
[35] J.-L. Pichard and G. Sarma, J. Phys. C **14**, L127 (1981); **14**, L617 (1981).
[36] A. MacKinnon and B. Kramer, Phys. Rev. Lett. **47**, 1546 (1981).
[37] J.-L. Pichard, in *Quantum Coherence in Mesoscopic Systems*, edited by B. Kramer, NATO Advanced Studies Institute, Series B: Physics (Plenum Press, New York, 1991), Vol. 254, pp. 369–399.
[38] O. N. Dorokhov, JETP Lett. **36**, 318 (1982).
[39] P. A. Mello, P. Pereyra, and N. Kumar, Ann. Phys. (N.Y.) **181**, 290 (1988).
[40] E. Abrahams, P. W. Anderson, D. C. Licciardello, and T. V. Ramakrishnan, Phys. Rev. Lett. **42**, 673 (1979).
[41] G. Theodorou and M. H. Cohen, Phys. Rev. B **13**, 4597 (1976).
[42] P. Markoš, Z. Phys. B: Condens. Matter **73**, 17 (1988).
[43] P. Markoš and L. Schweitzer, J. Phys. A **39**, 3221 (2006).
[44] T. Ohtsuki, K. Slevin, and Y. Ono, J. Phys. Soc. Jpn. **62**, 3979 (1993).